Spatiotemporal intracellular calcium dynamics during cardiac alternans

```
1.) \blacktriangle 2

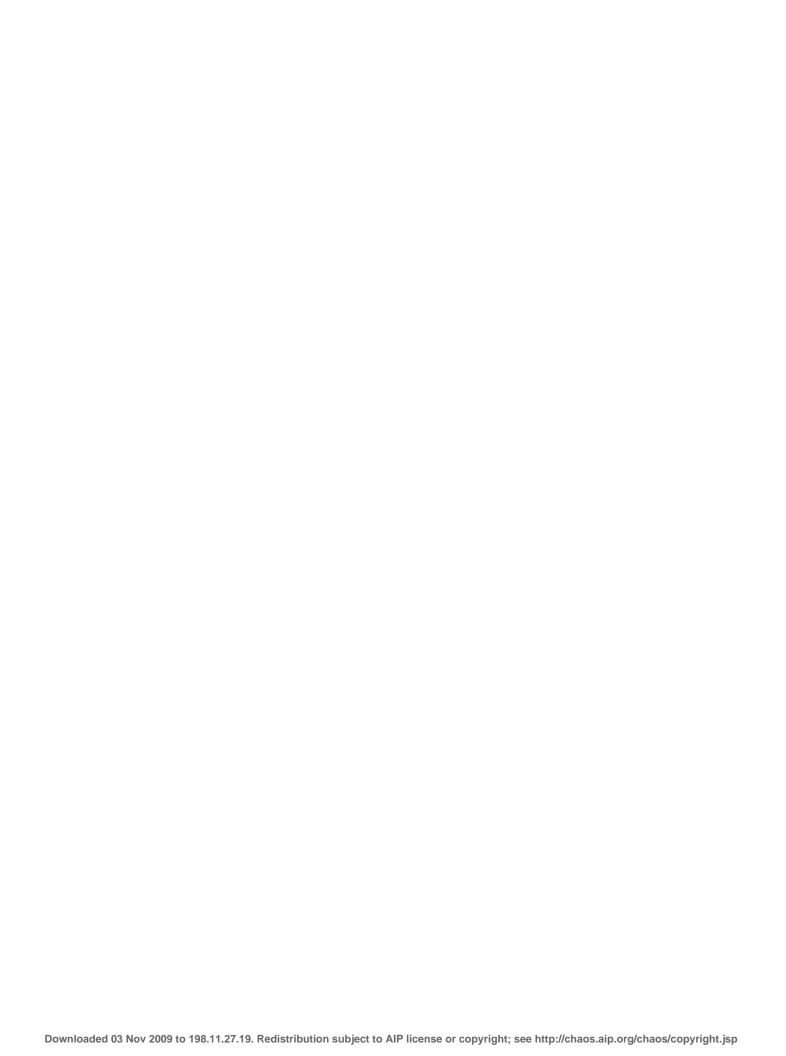
1 De a e f A ied Mahe aic, U i e i f C ad, B de, C ad 80309, USA
2 De a e f Ph ic a d Ce e f I e dici i a Reeach i C e S e,
N hea e U i e i, B , Ma ach e 02115, USA
```

(Received 30 June 2009; accepted 28 July 2009; published online 18 September 2009)

Cellular calcium transient alternans are beat-to-beat alternations in the peak cytosolic calcium concentration exhibited by cardiac cells during rapid electrical stimulation or under pathological conditions. Calcium transient alternans promote action potential duration alternans, which have been linked to the onset of life-threatening ventricular arrhythmias. Here we use a recently developed physiologically detailed mathematical model of ventricular myocytes to investigate both stochastic and deterministic aspects of intracellular calcium dynamics during alternans. The model combines a spatially distributed description of intracellular calcium cycling, where a large number of calcium release units are spatially distributed throughout the cell, with a full set of ionic membrane currents. The results demonstrate that ion channel stochasticity at the level of single calcium release units can influence the whole-cell alternans dynamics by causing phase reversals over many beats during fixed frequency pacing close to the alternans bifurcation. They also demonstrate the existence of a wide range of dynamical states. Depending on the sign and magnitude of calciumvoltage coupling, calcium alternans can be spatially synchronized or desynchronized, in or out of phase with action potential duration alternans, and the node separating out-of-phase regions of calcium alternans can be expelled from or trapped inside the cell. This range of states is found to be larger than previously anticipated by including a robust global attractor where calcium alternans can be spatially synchronized but out of phase with action potential duration alternans. The results are explained by a combined theoretical analysis of alternans stability and node motion using general iterative maps of the beat-to-beat dynamics and amplitude equations. © 2009 A e ica I i e f Ph ic . [DOI: 10.1063/1.3207835]

The con cile machine of a hea ell i acin el b be cor io elea e of calci m f om in cell la e. Thí elea e ca e be calci m concen sien of i e 🚜 n ien 🌉 and 🌬 n dec ea e a calci m i 🕴 m 🖰 ed back in orbre orbe a ailable foelea e a trans ne treat Thi "calci m c cling' in and o af be can ben able, i be be ne e l be be come d namicall f eak calci m concen ion al e na e f om bea bea The e f e iod- o cilla in, kno n a "calci m nien de man', ha e been linked og by on e of life-bea eting hea h ban di o de . 1,2 The haire ah oald namic of in cell la calci m d ing al e nan, ho e e , i i fa f om being f ll e f lo ed. Thi d namic i made e f eciall ich b be fac and memb ane olare a e bidi ec imall co f led. Calci m en in orbe cell ia ol are ga et L-re calci m

co3 9i -413i 7ŤJŤ(a)17.9(e)-420.1(mo)17.9(e)-420.1(idel)-420.1(kno n)-420.1(o) 420.1(be)-420.1(ei b.)-402.2(in)-420.1(o



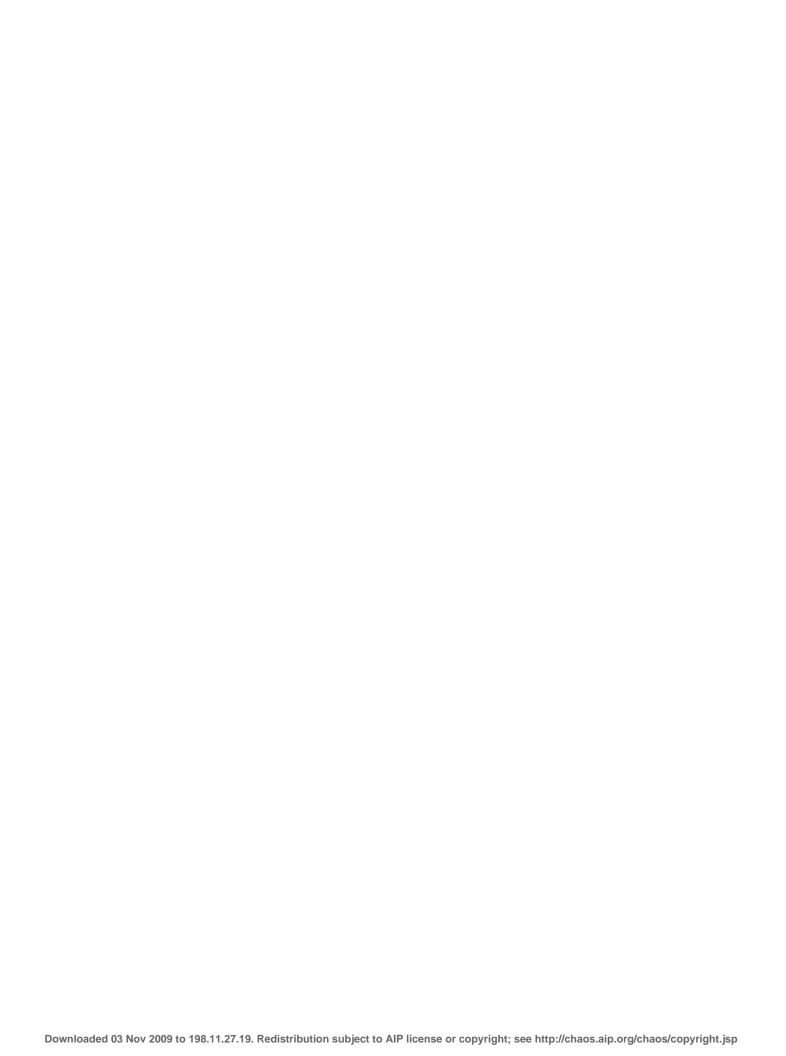
II. BACKGROUND

A. Excitation-contraction coupling

Here we briefly summarize the dynamical processes by which the membrane depolarization signal is relayed to the contractile machinery of the cell, named *e ci a i - c ac i c i g*. For a thorough review of excitation-contraction coupling, see, for example, Ref. 3.

When a myocyte is electrically excited by neighboring cells, voltage sensitive ion channels open, triggering a temporary (~200 ms) depolarization of the membrane from its resting potential, about -80 to 20 mV. This ac i is the result of the activation and subsequent inactivation of various ionic currents which transport mostly calcium, potassium, and sodium across the membrane. The depolarization of the membrane triggers influx of calcium into the cell through the LCCs. These channels are localized close to the terminal compartments of an internal saclike structure [sarcoplasmic reticulum (SR)] that stores calcium inside the cell. These terminal compartments have a cluster of about 100 calcium sensitive channels [ryanodine receptors (RyRs)] which open when the nearby calcium concentration increases. They, in turn, release even more calcium from the SR, raising the calcium concentration inside the cell and activating its contractile machinery. Subsequently, calcium is both reuptaken into the SR and extruded from the cell in preparation for the next stimulus.

A few LCC channels and $\sim \! 100$ RyRs are clustered in CRUs that are distributed in a three-dimensional (3D) grid across the myocyte, so as to guarantee a uniform calcium release across the volume of the cell



The model can be simulated using two different methods which correspond to commonly used experimental protocols. The calculus applied, initiating an action potential by the activation of inward ionic currents. In the calculus ed protocol, the membrane potential is forced to be a prescribed periodic signal, the large calculus age calculus applied. In the simulations, we obtain this signal by averaging the unclamped case membrane potential over many beats, so that the voltage clamp

beats $c_2 - c_{2-1}$, measured on even beats. The time between consecutive phase reversals can be as large as ~900 beats (e.g., horizontal bar in the clamped, T=325 ms panel of Fig. 5). At a critical period T, the time between phase reversals diverges and a well defined phase for alternans prevails. These results are in contrast to those in previous models of calcium alternans, where the peak calcium concentration undergoes a period doubling bifurcation in a deterministic way. 20 A signature of calcium fluctuations that could be detected experimentally is that due to calcium-voltage coupling, the action potential duration exhibits fluctuations that track those in the calcium concentration. In Fig. 6 we show the action potential duration (thin lines) and peak calcium concentration (thick lines) at even and odd beats for simulations corresponding to the unclamped, T=345 ms panel in Fig. 5, showing how fluctuations in the action potential duration track the fluctuations in peak calcium concentration during a phase reversal. If the alternans are voltage driven, we expect that there would be almost no fluctuations in the action potential duration alternations, since fluctuations in membrane ion channels are averaged out by the long range voltage coupling of these channels. Even though there is still a feedback from the calcium dynamics which could introduce fluctuations in action potential duration alternations, the dominant component of the alternans is almost deterministic and thus we expect fluctuations to be much smaller.

Of particular interest is the calcium dynamics that mediates the phase reversals. In the spatial model, a phase reversal occurs as domains with opposite phase to the whole-cell alternans phase grow due to fluctuations and eventually become dominant. Similar spatiotemporally complex subcellular discordant alternans have been observed experimentally, and we find that they are common during the spontaneous phase reversals of calcium alternans.

Because CRUs are heterogeneous (in the model, as in real myocytes, they have heterogeneous volumes)

CRUs with longitudinal coordinate smaller than 3/5 of the longitudinal extension of the myocyte. This induces larger release in those CRUs during one beat, creating two regions with calcium alternans of opposite phase. We then track the movement of the node separating these regions by calculating the transversal calcium average $c_T(J, \cdot)$, defined as the average of peak calcium $c^{(\cdot)}$ in beat—over all the CRUs which share the same J^{th} longitudinal coordinate (see Fig. 9). The position of the node along the longitudinal direction of the cell at beat—is then defined as the coordinate—such that $c_T(\cdot,\cdot) = c_T(\cdot)$, where $c_T(\cdot)$ is the spatial average of $c_T(J,\cdot)$ and—is found by interpolation of the function $c_T(J,\cdot)$ evaluated at discrete values of J.

In order to explore different dynamical regimes, we vary some of the parameters of the cellular model. In Appendix A we introduce parameters γ_{NCX} and γ_{Ca} that control the strength of the calcium current (I_{Ca}) and the sodium-calcium exchanger current (I_{NCX}). In addition, in Appendix A we also introduce two parameters α_{NCX} and α_{Ca} representing the ratio of effective membrane capacitance for the NCX and I_{ca} currents to that of the other membrane currents, which depends on the area distribution of ion channels in the external membrane and the T tubules²⁹ (see Appendix A). These parameters modify the effect of I_{Ca} and I_{Ca} and I_{Ca} (10552)



instability causes period doubling oscillations of the calcium concentration to develop out of phase in two halves of a cell. In Ref. 8, the existence of this instability was demonstrated using a physiologically detailed 1D model of bidirectionally coupled voltage and calcium dynamics, where CRUs with deterministic dynamics are spatially distributed along the length of the myocyte.

Our present simulations confirm the existence of a Turing instability for fast pacing rate and parameters where SCA are EMD, as predicted in Ref. 8. Stochasticity provides a natural mechanism to trigger the instability but does not alter fundamentally the development of the instability in a strongly nonlinear regime when alternans have a large enough amplitude. One new finding, however, is that EMD alternans can also occur for parameters where the Turing instability is absent. In contrast, in Ref. 8, it was concluded that the condition for the occurrence of a Turing instability was the same as the one for the occurrence of EMD alternans, in apparent disagreement with our finding. Here we revisit the iterative map based stability analysis of alternans of Ref. 8 to resolve this disagreement. To help us interpret our simulation results, we also derive predictions for the motion of the node separating out-of-phase regions and characterize the nonlinear character of the alternans bifurcation in the case of negative voltage-calcium coupling. We conclude at the end of this section that this disagreement is a consequence of a simplifying assumption made in Ref. 8. Relaxing this assumption leads to the prediction that the condition for the occurrence of EMD alternans is distinct from the one for the occurrence of a Turing instability, and hence EMD alternans can exist as a global attractor of the dynamics.

A. Stability of period one state against spatially concordant and discordant perturbations

The starting point of our analysis is the general map of the beat-to-beat dynamics describing the spatially concordant state where calcium alternans have the same amplitude and phase across the myocyte,

$$A = f_1(A_{-1}, c_{-1}), (1)$$

$$c = f_2(A_{-1}, c_{-1}), (2)$$

where A and c are the action potential duration and the

$$\lambda_c^- \approx J_{22} - \frac{J_{12}J_{21}}{J_{11} - J_{22}}. (9)$$

Since $A\sim (\lambda_c^\pm)\sim (-1)~e^{-\ln(-\lambda_c^\pm)},$ and similarly for c , alternans forms when λ

alternans is unstable to both SDA and SCA perturbations, and the question arises as to what nonlinear state is dynamically selected. As shown in Appendix C, the nonlinearly saturated SCA state is unstable for $|J_{12}J_{21}/(J_{11}-J_{22})| < |1+J_{22}| < (3/2)|J_{12}J_{21}/(J_{11}-J_{22})|$ and stable for

$$|1 + J_{22}| > (3/2)|J_{12}J_{21}/(J_{11} - J_{22})|. (13)$$

The nonlinearly saturated SDA state, in turn, is stable for $|1+J_{22}|\!>\!0$. Thus if condition (13) is satisfied, and $J_{12}J_{21}$ $<\!0$, both SDA and SCA are stable nonlinear states. Since the voltage-calcium coupling $|J_{12}J_{21}/(J_{11}-J_{22})|\!\ll\!1$ in our simulations, these two states are always bistable except in a negligible parameter range very close to the alternans bifurcation. This bistability leads to a nonuniqueness of the dynamically selected state for negative coupling that has been noted in previous studies of coupled cells and tissue. $^{33-35}$

The analysis of the weak negative coupling limit makes

stochastic effects account for the drifting node motion in the unclamped case. The clamped simulations have a perfectly periodic voltage, which implies $J_{12} \equiv 0$. Thus, Eq. (12) predicts no node motion in the clamped case, in agreement with the observations in Ref. 6. However, fluctuations result in drifting motion of the node as observed in Fig. 10. This drifting motion might eventually lead to SCA if the node is expelled due to its drifting motion.

Fifth, we have found that SCA can develop with voltage alternans in or out of phase with calcium alternans. As we have seen, this is consistent with the prediction that spatial synchronization requires $J_{12}J_{21}>0$, while the relative phase of voltage and calcium alternans is governed by the sign of J_{12} in Eq. (11). This prediction is simplest to understand by noting that the peak calcium transient amplitude is determined predominantly by the peak amplitude at the previous beat, and more weakly by the voltage history. Thus J_{12} can be approximated using the chain rule as $J_{12} \approx (\partial A / \partial c)$ $\times (\partial c / \partial c_{-1})$. Since $\partial c / \partial c_{-1} = J_{22} < 0$, J_{12} is negative only if $\partial A / \partial c < 0$, or when a larger peak calcium transient amplitude produces a shorter action potential duration. This is expected to occur when the balance between LCC and NCX is shifted toward LCC, consistent with the observation that voltage and calcium alternans are out of phase in our simulations when NCX is reduced by 80% of its normal value (cases B and D).

Let us contrast our present results with those of Ref. 8. In Ref. 8, it was concluded that SDA can only develop under

increase the amplitude of calcium alternans, thereby mediating a positive feedback of calcium alternans on itself. In contrast, for negative coupling, voltage alternans tend to suppress calcium alternans, thereby mediating a negative feedback of calcium alternans on itself. Mathematically, the coupling is determined by the product of the off-diagonal terms J

and within the compartments of the SR. I_{ci} , I_c , and I_{cNSR} are diffusive currents coupling the cytosolic, submembrane, and network SR compartments of adjacent CRUs (three lower arrows in Fig. 3). The calcium current I_{Ca} and the sodium-exchanger current I_{NCX} are calcium transmembrane currents

$$\left(\delta - 3 c^2 + D \frac{\partial^2}{\partial^2}\right) c \equiv \mathcal{L}c = -v \frac{\partial c}{\partial} - \kappa c,$$
 (B9)